Article

Journal of the Brazilian Chemical Society

https://dx.doi.org/10.21577/0103-5053.20240158

J. Braz. Chem. Soc. **2025**, *36*, 3, e-20240158, 1-12

In vitro and *in silico* Antifungal Activity of Metabolites from *Bredemeyera brevifolia* (Benth.) Klotzsch ex A.W. Benn.

Rubens S. Barreto, [*,a,b] ***Diego M. da Costa,*** [a] ***Jailan S. Sousa,*** [c] ***Vilisaimon S. de Jesus,*** [d] ***Agnaldo P. da Silva,*** [c,e] ***Maria Daniela S. Buonafina-Paz,*** [f] ***Franz A. G. dos Santos,*** [g] ***Rejane P. Neves,*** [f] ***José F. B. Pastore,*** [h] ***Bruno S. Andrade,*** [c] ***Wagner R. A. Soares,*** [c] ***Hugo N. Brandão,*** [a] ***Rosane M. Aguiar*** [d] ***and Clayton Q. Alves*** [a]

[a]*Programa de Pós-Graduação em Recursos Genéticos Vegetais (RGV), Departamento de Ciências Biológicas, Universidade Estadual de Feira de Santana, 44036-900 Feira de Santana-BA, Brazil*

[b]*Departamento de Ensino, Instituto Federal de Educação, Ciência e Tecnologia da Bahia, 45201-767 Jequié-BA, Brazil*

[c]*Laboratório de Bioinformática e Química Computacional, Departamento de Ciências Biológicas, Universidade Estadual do Sudoeste da Bahia, 45200-000 Jequié-BA, Brazil*

[d]*Programa de Pós-Graduação em Química, Departamento de Ciências e Tecnologias, Universidade Estadual do Sudoeste da Bahia, 45200-000 Jequié-BA, Brazil*

[e]*Departamento de Posgrado, Corrientes 720 PB y 1 er Piso, Instituto Universitário Italiano de Rosário, S2000CTT Argentina*

[f]*Departamento de Micologia, Universidade Federal de Pernambuco, 50670-901 Recife-PE, Brazil*

[g]*Departamento de Medicina Tropical, Universidade Federal de Pernambuco, 50670-901 Recife-PE, Brazil*

[h]*Herbário - CTBS, Universidade Federal de Santa Catarina, 89520-000 Curitibanos-SC, Brazil*

Bredemeyera Willd. is a genus of the Polygalaceae family, occurring in Brazil. This research aims to evaluate the phytochemical and antifungal potential, *in vitro* and *in silico*, of *Bredemeyera brevifolia* extracts. The identification of fatty acids by gas chromatography-mass spectrometry and their quantification by gas chromatography-flame ionization detector showed that palmitic (36.55 mg g^{-1}), margaric (3.66 mg g^{-1}), linolelaidic (108.82 mg g^{-1}), oleic (7.86 mg g^{-1}), stearic (41.11 mg g^{-1}), dihomo-γ-linolenic (85.48 mg g^{-1}), and arachidic (209.00 mg g^{-1}) acids are present in the hexane extract. From the chloroform extract, 1-hydroxy-3,7-dimethoxyxanthone was isolated and identified. The minimum inhibitory concentration assay with methanolic extract demonstrated antifungal activity against species of the genus *Candida*, *Sporothrix*, and *Trichophyton* for up to 96 h, with values ranging from 64-1024 μg mL^{-1}. The *in silico* study with the chemical compounds of this species showed fungal inhibition potential of sterol-14-α-demethylase, highlighting 1-hydroxy-3,7-dimethoxyxanthone, which presented an affinity energy of −8.8 kcal mol^{-1}, greater than that observed for fluconazole (−8.3 kcal mol^{-1}). The fatty acids interacted with the active site of the enzyme but presented energies ≥ −7.4 kcal mol^{-1}. Compounds isolated from this species have pharmacokinetic potential for the development of pharmaceutical formulations.

Keywords: *Bredemeyera brevifolia*, fatty acid, 1-hydroxy-3,7-dimethoxyxanthone, lanosterol 14-alpha demethylase, antifungal activity, molecular docking

Introduction

The Polygalaceae family has 27 genera, encompassing about 1.300 species distributed in different parts of the planet, mainly in temperate, hot, and tropical zones. About 11 genera of this family are found in Brazil, including the genus *Bredemeyera* Willd.[1] The use of plants of this genus in traditional medicine includes: fighting kidney inflammation, diarrhea, rheumatism, spine pain, and gastritis.[2]

*e-mail: rubensbarreto@ifba.edu.br
Editor handled this article: Paulo Cezar Vieira

Bredemeyera Willd. is still poorly studied, with only ethnobotanical studies of 3 of its species, *Bredemeyera brevifolia*, *B. floribunda*, and *B. laurifolia*. On the other hand, phytochemical investigations were conducted just with *B. brevifolia* and *B. floribunda.* From *B. floribunda*, the presence of triterpenoid saponins (bredemeyroside B, C and D), and xanthones (1,7-dihydroxy-3,4,8-trimethoxyxanthone, 1,3,7-trihydroxy-4,8-dimethoxyxantone) was verified. From *B. brevifolia* three xanthones were isolated and identified: 1-methoxy-2,3,7,8-dimethylenedioxyxanthone, 1,7-dihydroxy-3,4,8-trimethoxyxanthone, and 1,7,8-trimethoxy-2,3-methylenedioxyxanthone. In addition, palmitic, oleic, stearic, behenic, linoleic, and lignoceric acids were identified in its extract.[3-6]

Although there is no record of the popular use of *Bredemeyera* Willd. in the treatment of diseases or infections caused by fungi, two classes of substances isolated from *B. brevifolia*, xanthones and fatty acids have antimicrobial potential and their antifungal activities have been tested in search of new drugs.[7-9]

In vitro and *in silico* studies with xanthones and other substances have been used together to evaluate antimicrobial activity. Thus, it is possible to obtain a profile of the action of these substances with *in vitro* models using fungi of interest, as well as their physicochemical, pharmacokinetic and absorption, distribution, metabolism, excretion and toxicity (ADMETox) properties through *in silico* studies. The association of this information may be useful for the development of phytopharmaceuticals or semi-synthetic analogues with antifungal action.[10]

Considering the lack of information about the chemical and medicinal potential of the *Bredemeyera* species, this research aimed to carry out a phytochemical study of the methanolic extract from *B. brevifolia* leaves, in order to know the chemical composition, as well as to evaluate its *in vitro* and *in silico* antifungal activity against yeast, filamentous and dermatophyte fungi, thus contributing to the chemosystematics of this species, still little studied.

Experimental

General information

The chromatographic analysis was performed in a GC-2010 Plus Shimadzu apparatus (Shimadzu, Kyoto, Japan) with a flame ionization detector (FID) and an Rt-2560 fused silica capillary column (100 m, 0.25 mm internal diameter (i.d.)), with N_2 as a carrier gas and H_2 as an auxiliary gas, both supplied by White Martins (Salvador, Brazil). Gas chromatography-mass spectrometry (GC-MS) analysis was performed in a GC-QP2010 Shimadzu device (Shimadzu, Kyoto, Japan), using an SLB-5MS fused silica capillary column (30 m × 0.25 mm i. d.) × 0.25 μm (J & W Scientific company, Folsom, USA), coupled to an AOC-20i auto-injector, detector with electron impact ionization source (70 eV). One and two-dimensional nuclear magnetic resonance (NMR) analysis was performed, in an INOVA 500 Spectrometer (Varian company, USA), operating at 500 MHz (^{1}H) and 125 MHz (^{13}C), using tetramethylsilane (TMS) as an internal standard and $(CD_3)_2CO$ as a solvent (Merck, Darmstadt, Germany). Analytical standard fatty acid methyl esters (FAME)-Supelco 37 Component FAME Mix C4-C24 (Sigma-Aldrich, Bellefonte, USA). PA grade solvents and BF_3/methanol solution, all from Sigma-Aldrich and Merck.

Plant material

B. brevifolia leaves were collected at the Rio de Contas dam, in the municipality of Rio de Contas, Bahia-Brazil. The species were collected and identified in February 2018. The exsiccate was deposited in the Herbarium of the Botany Department of Universidade Federal de Santa Catarina, under number CTBS 3935. Access to the Brazilian national genetic heritage was registered in the National System for the Management of Genetic Heritage and Associated Traditional Knowledge (SisGen), according to the certificate of regularity of access number ADA5ACA.

Obtention of the organic extract

The dried and crushed leaves (439.24 g) were macerated in methanol (Synth, Salvador, Brazil). This process resulted in the formation of a *B. brevifolia* (BBB) alcoholic extract, weighing 137.53 g. The BBB extract was then subjected to further extraction using organic solvents: hexane, chloroform, and ethyl acetate (all provided by Synth, Salvador, Brazil). As a result, hexane (HBB, 8.44 g), chloroform (CBB, 17.38 g), and ethyl acetate extracts (AcBB, 10.29 g) were obtained.

Extraction and obtention of fatty acid (FA) methyl esters

HBB (1.00 g) was filtered in a chromatographic column (CC), using 20.0 g of silica gel 60 (Synth, Salvador, Brazil) as a stationary phase and chloroform as a mobile phase, resulting in a fraction called HBB-C (584.70 mg). HBB-C (10.00 mg) was dissolved in 100 μL of an ethanolic solution of 1.0 mol L^{-1} potassium hydroxide (5%) (Synth, Salvador, Brazil), and heated in a domestic microwave oven at 5% power for 15 min. Subsequently,

100 mL of water were added and successive extractions with hexane (3 × 300 mL) were performed. The aqueous phase obtained was acidified with HCl (1.0 mol L^{-1}) and the free FA were extracted with ethyl acetate (3 × 300 mL). The free FA were derivatized by esterification, with 100 µL of 14% BF_3/methanol, centrifuged for 15 min, and then placed in a water bath (80 °C) for another 15 min, enabling identification and quantification by GC-MS and GC-FID, respectively.

Identification and quantification of FA of HBB

The GC-MS identification process had specific chromatographic conditions, including 290 °C injector temperature, carrier gas flow rate of 1.8 mL min^{-1}, 260 °C detector temperature, and 290 °C interface temperature. The oven temperature program started at 100 °C min^{-1}, followed by a gradual increase at a rate of 5 °C min^{-1} until it reached 285 ºC, where it was maintained for an additional 42 min. Mass detector analysis was conducted at a range of 40 to 350 *m/z*.

Quantification was performed by GC-FID. The sample split ratio was 90:10. The injector and detector temperatures were 225 and 260 °C, respectively. The column temperature started at 140 °C for 5 min, followed by a ramp of 3 °C min^{-1} to 245 °C for 20 min. Injections were performed in triplicate and injection volumes were 1.0 µL. The fatty acid methyl esters were identified and quantified by comparing their chromatographic times and peak areas to those of an authentic standard FAME Mix C4-C24, injected under the same conditions as those of the sample.

Extraction, isolation and characterization of the xanthone in CBB

CBB (16.00 g) was subjected to CC on silica gel 60, having hexane-acetone as a mobile phase in increasing polarity gradients. 115 fractions were obtained, which were later grouped by similarity into 7 fractions after thin-layer chromatography (TLC) analysis (Synth, Salvador, Brazil) revealed in vanillic acid.

The CBB-2 fraction (3.17 g) was subjected to CC filtration, using Sephadex LH-20 as a stationary phase and CH_2Cl_2:MeOH (1:1) as a mobile phase; 9 fractions were obtained. Among these, the fraction CBB-2B (2.98 g), that was fractionated in CC on silica gel, with $CHCl_3$:$(CH_3)_2CO$ in increasing polarity gradient, resulting in the purified substance **8** (10.00 mg), whose structure was identified after analysis of NMR data (one- and two-dimensional), as well as comparison with literature data.

In vitro tests

Filamentous fungi and yeasts

The strains used were obtained from the Research Group Fungi of Medical Interest and Yeasts of Biotechnological Interest, Department of Mycology, Federal University of Pernambuco. Clinical isolates of the genera *Candida* (*C. albicans*, *C. tropicalis*, *C. parapsilosis* and *C. krusei*), *Aspergillus* (*A. fumigatus*), *Trichophyton* (*T. rubrum*, *T. mentagrophytes* and *T. tonsurans*) and *Sporothrix* (*S. schenckii* and *S. brasiliensis*), resistant to azoles, in addition to a strain from the American Type Culture Collection (ATCC) (*Candida albicans* 14053, *Candida tropicalis* 750, *Candida parapsilosis* 22019, *Candida krusei* 6258 and *Aspergillus fumigatus* 204305) were used.

Antifungal preparation, bioproducts and culture medium

The experiment followed Clinical and Laboratory Standards Institute (CLSI) documents M27-A3 and M38-A2.[11,12] The stock solution of the antifungal fluconazole (Pfizer, Brazil) was prepared and diluted in Roswell Park Memorial Institute (RPMI) 1640 medium (Sigma-Aldrich, USA), with concentrations ranging from 64 to 0.125 µg mL^{-1}. The BBB was diluted in dimethyl sulfoxide (DMSO) (1%) (Synth, Salvador, Brazil) and 3.5 mL of RPMI, totaling 4 mL (solvent/RPMI); concentrations ranged from 2048 to 4 µg mL^{-1}. The culture medium used was RPMI 1640, with L-glutamine and sodium bicarbonate, pH 7.0 ± 0.1. Preparation took place in deionized water, sterilized at 46.5 g L^{-1} and buffered with morpholino propane sulfonic acid (MOPS 0.165 mol L^{-1}; Sigma-Aldrich, USA). Sterilization was performed in a biological filter (Nalgene Company, Rochester, USA), using a 0.22 µm membrane (Millipore, Darmstadt, Germany).

Preparation of the inoculum for the sensitivity test

Yeasts and filamentous fungi were grown on Sabouraud Dextrose Agar and Potato Dextrose Agar, respectively. They were kept at 35 ºC for 24 and 120 h, respectively, according to CLSI documents M27-A3 and M38-A2.[11,12] An initial inoculum suspension was prepared in 5 mL of sterile saline solution (NaCl; 0.85% saline) and its density was adjusted according to the McFarland scale, 0.5 with transmittance of 90% for yeast and 70-80% for filamentous fungi determined by spectrophotometry, using a compression wave of 530 nm. This procedure provided a standard concentration of yeast containing 1×10^6 to 5×10^6 cells mL^{-1}, followed by 1:100 dilution and then 1:20 dilution of the standard suspension with RPMI 1640

medium for yeasts and 1:50 for filamentous fungi, resulting in the concentration from 5.0×10^2 to 2.5×10^3 cells mL^{-1}, grown at 37 °C.

Broth microdilution test

Microdilution was performed in flat bottom plates (TPP, Trasadingen, Switzerland) with 96 wells and eight series distributed from A to H (vertical), each with 12 wells (horizontal). From the antifungal stock solution and the by-product obtained from the BBB, solutions ten times the desired final concentration were prepared. For fluconazole, 0.125-64 μg mL^{-1} were used, and for the by-product, 4-1048 μg mL^{-1}. In the microdilution plates, 100 μL of each concentration were placed. Subsequently, these were kept at –20 ºC until the test, without exceeding the period of 30 days. On experiment days, plates were used after 30 min at 25 °C. At different concentrations of antifungal and by-product in the plate wells, 100 μL of strain suspensions of the genus *Candida*, *Aspergillus*, *Trichophyton* and *Sporothrix* were tested. The tests were performed with a positive control containing 12 antifungal diluents and half-inoculum solution in the wells, in addition to a negative control containing some of column 11 antifungal solution and half-inoculum and the negative control containing only RPMI 1640 medium well in the column. The plates were kept in an oven at 35 ºC for up to 96 h, depending on the species. After this period, the test plates were observed and subsequently interpreted.

Data analysis

In the readings, the growth in the positive control well (12 column wells) was visually compared with the lowest concentration capable of inhibiting growth in relation to the different concentrations tested (wells 1 to 10). The criteria to define sensitivity to resistance were defined according to the protocol of documents M27-A3, M60 and M38-A2;[11,12] for fluconazole, a minimum inhibitory concentration (MIC) ≤ 8 μg mL^{-1} was accepted as reasonable and, in cases where MICs were 16 and 32 μg mL^{-1}, they were considered dose-dependent. MIC values above the mentioned numbers were indicated as resistant. The BBB MIC was evaluated according to documents M27-A3 and M38-A2. Determination was based on the lowest concentration that inhibited growth.

Visual reading

After determining the BBB MIC against *Candida* spp., *Aspergillus* sp., *Sporothrix* sp. and *Trichophyton* sp., the minimum fungicidal concentration (MFC) was determined to assess the ability to recover fungal growth after 48 h of contact with the test substance. With the aid of a sterile pipette, 10 μL of the mixture from each well were added to Sabouraud Dextrose Agar. The plates were incubated at 37 ºC for up to 96 h, according to the fungal species and, after incubation, it was observed if there were fungal growth.

In silico experiments

Drugbank searching

A search on the DrugBank database was performed with the keywords: "antifungal azole drugs", where only drug structures that selectively acted on lanosterol-14-α-demetilase were selected. The selective synthetic inhibitors for lanosterol-14-α-demetilase developed by the pharmaceutical industry were selected in the literature.

Dataset, virtual screening, molecular docking and ADMETox tools

All molecules were checked and designed using the Marvin Sketch™ software.[13] The molecular structures were downloaded in SMILES format and afterwards, using the Open babel™ software,[14] they were converted to a 3D sdf format for docking calculations. The sterol-14-α-demethylase crystallographic structure (5ZT1) was obtained from the Protein Data Bank (PDB).[15] All docking simulations were performed with the AutoDock Vina™ software.[16] Docking was performed between the proposed ligands: **8**, lanosterol, fatty acids (**1-7**), antifungal azole drugs and the receptor, which was prepared and converted to a pdbqt format using AutoDock™ tools software.[16] Docking results and the evaluation of each receptor-ligand complexes, such as affinity energy (kcal mol^{-1}) and ligand positioning inside the sterol-14-α-demetilase active site were analyzed using the PyMOL 2.1™ software.[17] Nine ligand poses were generated for each complex and returned their respective affinity energies. Subsequently, all best selected ligand-protein poses were graphically represented using PyMOL 2.1™,[17] and their respective 2D interaction maps were generated using the Discovery Studio 4.5™ software.[18] The ADMETox properties were evaluated by the Data Warrior™ and PkCSM™ softwares.[19,20]

Molecular dynamics of 5TZ1 ligand-free (APO)

All the molecular dynamics simulations were carried out using the program package GROMACS,[21] along with Charmm36 force field.[22] Initially, the system was solvated with (TIP3P) water embedded in the simulation boxes and then neutralized by adding three sodium ions. Subsequently, the system was subjected to a steepest descent energy minimization until the maximum force reached less than 1000 kJ mol^{-1} *per* nm. The whole system was gradually

relaxed and heated up to 310 K after equilibrating with the fixed protein at 310 K. Finally, 50 ns molecular dynamics (MD) simulations were performed under normal temperature and pressure. Therefore, the GROMACS[21] utilities were used in order to obtain the root mean square deviation (RMSD), root mean square fluctuation (RMSF), hydrogen bond, and interaction energy. All the plots were done by Xmgrace software (Grace-5.1.25).[23]

Molecular dynamics of 5TZ1 and 1-hydroxy-3,7-dimethoxy-xanthone

Xanthone was parameterized with CGenFF web server.[24] The complex was then immersed in a dodecahedron box of TIP3P water molecules. The simulated system was neutralized by adding three sodium ions. The simulation and entrance system consisted of 5TZ1 protein, the xanthone, three sodium ions and 18747 water molecules. Energy minimization was performed by using the steepest descent method for 50000 steps; after that, the protein and ligand complex were equilibrated (at 300 K) and submitted to production (at 50 ns) phase, following normal temperature and pressure conditions.

Results and Discussion

Identification and quantification of FA in *B. brevifolia* hexane extract

The FA composition present in the HBB was identified by GC-MS analysis (Figure S1, Supplementary Information (SI) section) of the corresponding methyl esters, obtained by classical chromatographic procedures and derivatization reactions. The retention times were correlated to those obtained in the FAME pattern analysis, under the same chromatographic conditions, being confirmed by *m/z* and fragmentation patterns, observed in MS. Table S1 (SI section) presents the composition of FA identified from HBB: palmitic (**1**), margaric (**2**), linolelaidic (**3**), oleic (**4**), stearic (**5**), dihomo-γ-linolenic (**6**) and arachidic (**7**) acids. The GC-FID analysis allowed the quantification of FA, through the correlation of peak areas, compared to those observed for the FAME pattern, with the major constituents represented by: **7** (209.00 mg g^{-1} HBB), **3** (108.82 mg g^{-1} HBB) and **6** (85.48 mg g^{-1} HBB). The sum of quantified masses for FA makes up 49.25% of the mass of HBB. In another study, only oleic, stearic and palmitic acids were identified in *B. brevifolia* hexane extract, without their quantification.[6]

Structural identification of the xanthone

The compound 1-hydroxy-3,7-dimethoxyxanthone (**8**) was obtained as an amorphous yellow solid, and its structural elucidation was carried out through the analysis of ultraviolet (UV), infrared (IR), and NMR (one- and two-dimensional) data. From these data, it was observed that the substance did not have a high degree of purity, as the spectra obtained from the techniques showed interfering signals of low intensity, which were isolated to avoid hindering the identification of the xanthone. Considering this factor, and the mass obtained (10 mg), it was not possible to perform the *in vitro* antifungal test with compound **8**. The UV spectrum revealed maximum absorption at ν_{max} 208, 245, 277 and 308 nm.[25,26] IR analysis (Figure S2, SI section) showed absorption bands at ν_{max} 1653 cm^{-1} (νC=O), characteristic of stretching of doubly conjugated carbonyl in an aromatic system.[27] The absorption bands at ν_{max} were 1215, 1165, 1118 cm^{-1} (νC–H) and 3435 cm^{-1} (νO–H), consistent with the O–H group attached to the aromatic structure.[27] The absorption bands at ν_{max} 1454, 1498 and 1594 cm^{-1} (νC=C, ArH) and at ν_{max} 3000 cm^{-1} (νCsp^2_H), confirm the presence of the aromatic system. In addition, the absorption bands at ν_{max} 810 and 680 cm^{-1} (δC–H, ArH) indicate its pattern with two C–H bonds and the angular deformations of ethers in the regions at 1272 and 1036 cm^{-1} (δC–O), characteristic of the aryl-ether- aryl fragment of the molecule.

The analysis of the hydrogen (^{1}H), carbon 13 (^{13}C), heteronuclear multiple bond correlation (HMBC), and heteronuclear multiple quantum coherence (HMQC) NMR spectra (Table S2; Figures S3-S5, SI section) allowed its structural identification. In the ^{1}H NMR spectrum, it was possible to observe two signals related to methoxyls in δ_H 3.88 and δ_H 3.93 (s). Five aromatic proton signals, whose couplings suggest the presence of two aromatic rings: the signals in δ_H 6.32 and δ_H 6.66 (d, *J* 2.0 Hz), were assigned to aromatic ring hydrogens with coupling in meta (ring A) and signals in δ_H 7.0 (d, *J* 8.0 Hz), δ_H 7.60 (dd, *J* 8.0/2.0 Hz) and δ_H 7.72 (sl), assigned to the coupling of the hydrogens of the trisubstituted aromatic ring (ring B). The presence of a singlet in δ_H 12.77 (s) was also observed, which was assigned to the chelatogenic hydroxyl at C-1.[28] The association of information from the ^{13}C, HMQC and HMBC NMR spectra (Table S2) allowed the unequivocal attribution of the positions of hydrogenated aromatic carbons, as well as the methoxyl and hydroxyl substituents in the structure (Figure S6). Data were compared to the spectrometric data observed in previous records[7,29] of substance **8**, allowing to identify this substance as 1-hydroxy-3,7-dimethoxyxanthone. Although its identification in other plant species has already been reported, this is the first report of its isolation from *B. brevifolia*.

Evaluation of the antifungal activity of extracts of *B. brevifolia*

The BBB demonstrated *in vitro* antifungal and fungicidal action, verified by obtaining the MIC. The BBB inhibited 100% of *Sporothrix* species with MIC ranging from 256 to 1024 μg mL^{-1}. Among dermatophyte fungi, there was inhibition against *Trichophyton rubrum* and *T. tonsurans* (1024 μg mL^{-1}). Among *Candida* species, inhibition occurred in 24 h in the range of 64 to 1024 μg mL^{-1}. It can be seen that wild *Candida* species had MIC higher than the MIC determined against standard strains, as shown in Table 1. MIC values lower than 1,000 μg mL^{-1} are considered satisfactory, which includes the MIC value of the BBB extract against the fungi used in this study.[30]

This is the first record of antifungal activity for *B. brevifolia*. The results observed in the *in silico* assay against lanosterol 14-alpha demethylase, a molecular target of biomedical interest for the development of new antifungals, demonstrated that the compounds isolated from the extracts of this species can be evaluated in future assays of antifungal action against drug-resistant strains.

Molecular docking, xanthone (XA), fat acids and drugs

The result of molecular docking indicates that xanthone (**8**) interacts with the amino acids of the active site of the enzyme compared to azole drugs, binding to 6 (tyrosine-118 (Tyr-118), tyrosine-132 (Tyr-132), glycine-307 (Gly-307), histidine-377 (His-377), serine-378 (Ser-378), and methionine-508 (Met-508)) of the 13 amino acid residues of the active site of 14-alpha-lanosterol-demethylase, important in the input and positioning for pre-catalysis and catalysis of substrates such as the lanosterol eburicol.[31] In terms of energy affinity, the xanthone (−8.8 kcal mol^{-1}) showed better affinity than fluconazole (−8.3 kcal mol^{-1}), a value that can be optimized with chemical modifications in the structure to achieve better affinity.

The analysis of fatty acids reveals that they effectively interact with the active site of the enzyme, crucial for maintaining fungal membrane integrity, and resisting new antifungal agents. These compounds also impact the essential Heme group, necessary for metabolite transport by the CYP51 enzyme. Although their affinity energy is slightly lower than that of fluconazole (Table S3, SI section), their flexibility and adaptability to the active site set them apart. Additionally, the high FA content in the extract enhances their activity in synergy with other compounds, as observed in the literature for fatty acids such as myristic and palmitic acids against systemic Candidiasis.[8] Other studies suggest that polyunsaturated fatty acids (PUFAs) exhibit intrinsic antibacterial, antifungal, antiviral, antiparasitic, and immunomodulatory properties.[32] Specifically, oleic acid has shown promise as a therapy for *Candida* sp. infections, while long-chain unsaturated fatty acids may

Table 1. Minimum inhibitory concentration (MIC) assay of *Bredemeyera brevifolia* leaf extracts

Strains (yeast)	BBB (24 h) / (μg mL^{-1})	Fluconazole (24 h) / (μg mL^{-1})
C. albicans (ATCC14053)	64 (100%)	0.5
C. albicans (MM 46)[a]	512 (100%)	0.5
C. krusei (ATTC6258)	128 (100%)	2.0
C. krusei (MM 06)[a]	512 (100%)	2.0
C. parapsilosis (ATCC22019)	128 (100%)	0.5
C. parapsilosis (MM 01)[a]	1024(100%)	0.5
C. tropicalis (ATCC750)	256 (100%)	0.5
C.tropicalis (MM 55)[a]	512 (100%)	1.0
Strains (filamentous fungi)	BBB (48 h) / (μg mL^{-1})	Itraconazole (48 h) / (μg mL^{-1})
A. fumigatus (ATCC204305)	NI	4.0
S. brasiliensis (URM 8074)	1024 (100%)	4.0
S. brasiliensis (URM 7969)	512 (100%)	4.0
S. brasiliensis (URM 8078)	256 (100%)	2.0
S. schenckii (URM 8080)	256 (100%)	2.0
Strains (dermatophytic fungi)	BBB (96 h) / (μg mL^{-1})	Itraconazole (96 h) / (μg mL^{-1})
T. mentagrophytes (URM 6272)	NI	4.0
T. rubrum (URM 5905)	1024 (100%)	0.5
T. tonsurans (URM 5508)	1024 (100%)	2.0

[a]Clinical strains collected from patients with systemic resistant infections admitted to the intensive care unit (ICU) at Hospital de Pernambuco. BBB: methanolic extract of *Bredemeyera brevifolia* leaves; NI: no inhibition.

influence the susceptibility and viability mechanism of itraconazole against *Aspergillus fumigatus*.[9,33]

Some authors[34] suggest that mutations in the amino acid Tyr-132 may be directly associated with the resistance mechanism of *Candida* sp. to fluconazole, a drug used as a model in microbiological assays of fungal inhibition. The investigated natural compounds (xanthone and FA) have an affinity with this amino acid, with van der Waals bonds different from those shown by fluconazole (Table S3). Fungal inhibition assays with the extracts were carried out in clinical *Candida* sp. strains resistant to azole drugs, being, therefore, promising in strategies involving the modeling of these molecules to improve their intermolecular affinity characteristics in the active site of the enzyme present in these strains resistant to antifungal drugs.[35]

Although FA have around 20 carbons in their chemical structure and are longer when compared to xanthone (**8**), which has a lower molecular weight, they did not show better affinity energies. However, xanthone has aromatic nuclei in its structure that favor binding with amino acids in the hydrophobic site of the enzyme 14-alpha-lanosterol-demethylase, approaching with azole drugs in terms of chemical similarity. FA have been studied due to their inhibitory action against filamentous and yeast-like fungi (*Aspergillus* spp. and *Candida albicans*) and the indications of interactive activity in the active site of 14-alpha-lanosterol-demethylase may be the starting point to explore the potential of compounds isolated from *B. brevifolia* extract against fungi of biomedical interest.[8,9,36]

The *Polygalaceae* family has been studied as a recognized source of polyoxygenated xanthones, being considered a standard taxonomic chemomarker for the genus *Bredemeyera*.[5,6] These oxygenated compounds have antimicrobial potential described in other species rich in xanthones, such as species from the genus *Anthocleista*.[37] 1-Hydroxy-3,7-dimethoxyxanthone demonstrated antifungal activity against *Candida parapsilosis* with MIC of 200 μg mL^{-1}.[7] As there are no records of the antimicrobial activity of polyoxygenated xanthones and FA in species of the genus *Bredemeyera*, this study is the first record of the antifungal activity of extracts and compounds of this species. The understanding of the best molecular mechanism of interaction with these residues will allow building a library of xanthone and fatty acid analogues as a drug design strategy for compounds with promising inhibitory activity against azole drugs in the treatment of fungal infections.

Similar to commercial drugs and lanosterol (Figure 1), xanthone (**8**) has a strong interaction with Tyr-118 (Pi-Pi T-shaped), which has not been observed with most fatty acids, except arachidic acid. However, what can explain the strong interaction of xanthone are the carbon-hydrogen interactions with Gly-303 and Gly-307 residues (Figure 1) present in helix I of the enzyme which, in turn, is related to the interaction with azoles,[38] in addition to the same type of interaction with Ser-378, not observed with commercial drugs, except for fluconazole (Table S3).

Therefore, the absence of strong interactions with these residues mentioned above and others such as Met-508, may explain the weak interaction of fatty acids, despite their lengths. All FA interact with His-377, a well conserved residue in fungi phylogeny, absent in human CYP51 proteins, which may confer a certain FA specificity by the fungal enzyme.[39]

The FA of *B. brevifolia* bind to the His-377 residue (Figure 1), with intermolecular energy of hydrogen bonds, stronger when compared to the van der Waals bond performed by lanosterol, a specific endogenous ligand of the enzyme sterol 14-α-demethylase.[38] FA have been investigated for their antifungal activity against yeast and filamentous fungi, with potential for building libraries of semi-synthetic analogues from natural structures with selective action for the molecular target.[8,9]

In silico prediction of ADMETox properties

The *in silico* predictions for the physicochemical and pharmacokinetic parameters of 1-hydroxy-3,7-dimethoxyxanthone and FA isolated from *B. brevifolia*, demonstrated that these compounds present good oral absorption and bioavailability, according to the Lipinski's rule of 05 (Table S4, SI section).[40] Xanthone showed a low topological polar surface area (TPSA), high intestinal absorption rate (95.14%) and a better lipid solubility profile (cLogP) when compared to fluconazole (81.52%) and lanosterol (89.97%).[39] Due to its high static distribution volume (VDss = –0.083) and high plasma protein binding, this molecule showed a high tissue distribution capacity, demonstrated by the low fraction of unbound drug in blood plasma (fraction unbound (Fu) = 0.126), when compared to fluconazole (Fu = 0.154). Thus, 1-hydroxy-3,7-dimethoxyxanthone has a promising profile for distribution in infected tissues, compared to fluconazole (Table 2).[41] The FA obtained from *B. brevifolia* showed physicochemical and pharmacokinetic behavior similar to lanosterol, drawing attention to the gastrointestinal absorption rate between 88.07-89.59%, high tissue distribution volume and low unbound fraction, approaching the physiological value of lanosterol. They did not present hepatotoxicity and showed a good renal excretion profile when compared to fluconazole and lanosterol (Table S4).

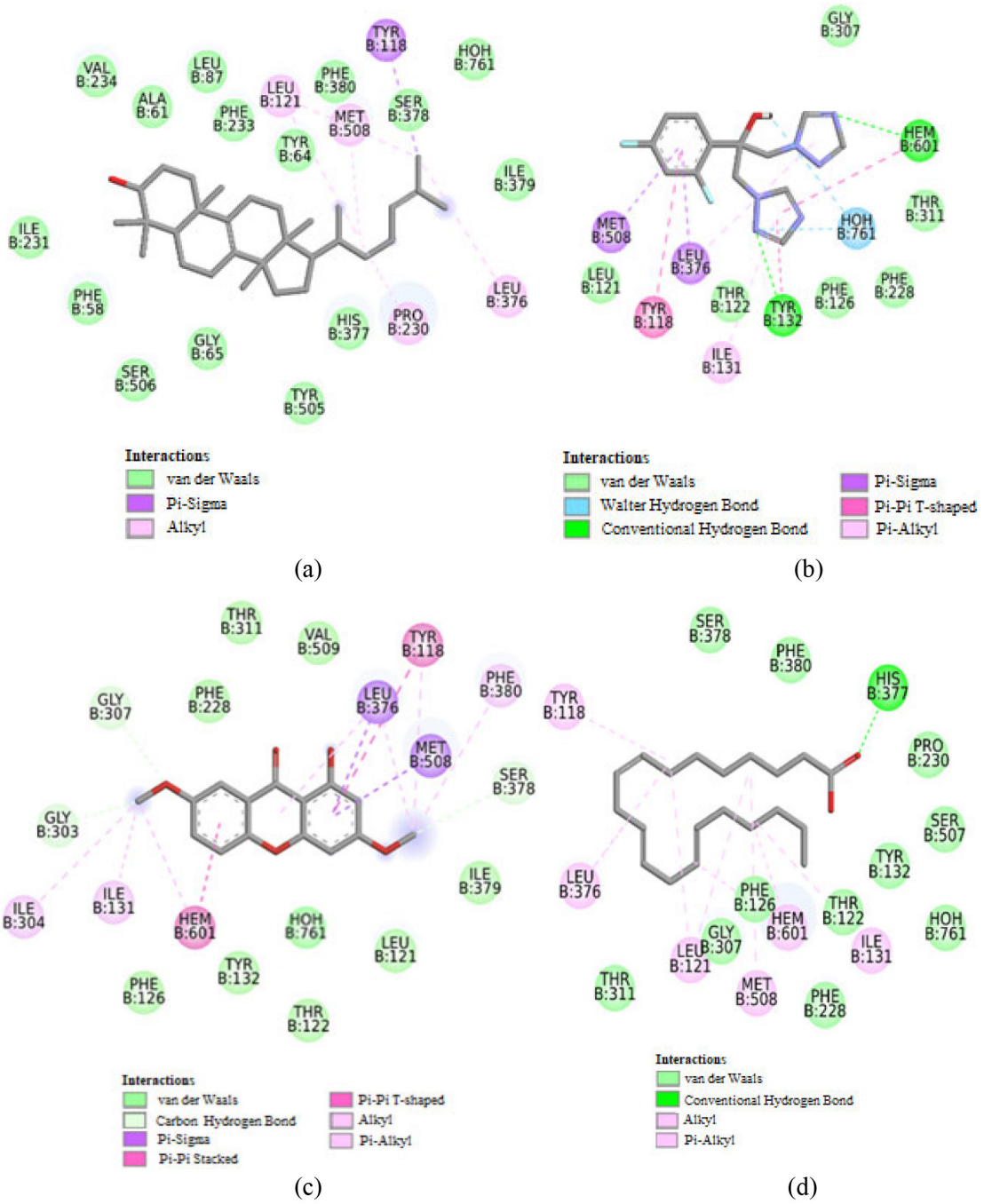

Figure 1. 2D interaction map between amino acids in the active site of sterol-14-α-demethylase with enzymes, patterns and constituents isolated from *Bredemeyera brevifolia*. (a) Lanosterol; (b) fluconazole; (c) 1-hydroxy-3,7-dimethoxyxanthone (**8**); (d) dihomo-γ-linolenic acid.

The compounds 1-hydroxy-3,7-dimethoxyxanthone and FA do not interfere with the enzymatic activity of CYP3A4, the main enzyme of the hepatic microsomal complex, responsible for metabolizing the vast majority of orally administered chemical substances, indicating an ease of biotransformation, and favoring detoxification and elimination from the body (Table 2).[42] 1-Hydroxy-3,7-dimethoxyxanthone, in particular, did not demonstrate hepatotoxicity and had a higher renal clearance rate (0.64 mg kg^{-1} *per* day), when compared to fluconazole (0.465 mg kg^{-1} *per* day), and may be more easily excreted. Due to their lipophilic characteristic, both xanthone and FA may undergo passive reabsorption in the renal tubules, which may favor their half-life ($T_{1/2}$), in addition to the biological life of these compounds in the body during the treatment of more persistent infectious processes (Table 2).

Metabolite production rate can increase or decrease according to the behavior of the compound, whether it is

Table 2. *In silico* pharmacokinetic properties for 1-hydroxy-3,7-dimethoxyxanthone, fat acids and other anti-fungal drug (sterol-14-α-demethylase) inhibitors

Molecule	Abs / %	VDss / (L kg^{-1})	Fu	1A2	2C19	2C9	2D6	3A4	Hept.	TC / (mg kg^{-1} *per* day)
Lanosterol	89.97	0.546	0	no	no	no	no	no	no	0.403
1-Hydroxy-3,7-dimethoxyxanthone	95.14	–0.083	0.126	yes	yes	yes	no	no	no	0.64
Fluconazole	81.52	–0.404	0.154	yes	no	no	no	no	yes	0.465
DHγL acid	89.59	–0.406	0.005	yes	no	yes	no	no	no	2.048
LNLD	89.77	–0.355	0.041	yes	no	yes	no	no	no	1.932
OLC acid	89.26	–0.323	0.04	yes	no	yes	no	no	no	1.88
ARQ acid	88.07	–0.316	0.009	yes	no	yes	no	no	no	1.896
EST acid	88.76	–0.292	0.039	yes	no	yes	no	no	no	1.828
MRG acid	89.10	–0.288	0.062	yes	no	yes	no	no	no	1.793
PMT acid	89.44	–0.289	0.091	yes	no	yes	no	no	no	1.759

Abs: percentage absorbed; VDss: static distribution volume; Fu: fraction unbound; 1A2 = CYP1A2; 2C19 = CYP2C19; 2C9 = CYP2C9; 2D6 = CYP2D6; 3A4 = CYP3A4: if molecule is a CYP inhibitor; Hept.: hepatotoxicity; TC: renal clearance; DHγL acid: dihomo-γ-linolenic acid; LNLD: linolelaidic acid; OLC acid: oleic acid; ARQ acid: arachidic acid; EST acid: stearic acid; MRG acid: margaric acid; PMT acid: palmitic acid.

an enzyme inducer or inhibitor. This behavior can affect the bioavailability profile of active substances or drugs, administered concomitantly during therapeutic treatment. In this case, xanthone demonstrated an inhibitory profile for CYP1A2 enzymes similar to fluconazole, being a substrate for metabolism through CYP2C19, CYP2C9, which may favor its elimination from the body.[43]

According to the toxicity profile, the values of oral rat acute toxicity (LD_{50}), maximum recommended tolerated dose in humans (MRTD) observed for 1-hydroxy-3,7-dimethoxyxanthone and FA are in a safe range for human ingestion, especially for the values of chronic oral toxicity in rats (LOAEL); when compared to fluconazole, natural compounds have a better safety range for use in chronic doses (Table 3).[44] As they are authentic chemical structures, the drug likeness (DL) and drug score (DS) values for 1-hydroxy-3,7-dimethoxanthone and FA differ from those presented by fluconazole, demonstrating potential for the development of new natural and semi-synthetic compounds derived from their natural chemical structures.[45]

Furthermore, 1-hydroxy-3,7-dimethoxanthone presented a mutagenic toxicity profile for xanthones in *Salmonella typhimurium* strains in the *in silico* prediction, besides toxicity for the reproductive system.[46] Fluconazole has also been reported to have a genomic variation effect that can induce fungal resistance.[47] The FA oleic acid, stearic acid and palmitic acid have demonstrated a mutagenic, tumorogenic and irritating toxicity profile, with no similar effects being observed in fluconazole. However, the use of this drug in clinical practice in resistant fungal infections

Table 3. Drug likeness, drug score and toxicity values for 1-hydroxy-3,7-dimethoxyxanthone, fat acids and fluconazole

Molecule	DL	DS	Mu	Tum	Rep	Irrit	LD_{50} / (mol kg^{-1})	LOAEL / (mg kg^{-1} *per* day)	MRTD / (mg kg^{-1} *per* day)
Lanosterol	–4.13	0.05	N	N	H	H	2.003	0.695	–0.84
1-Hydroxy-3,7-dimethoxyxanthone	–0.92	0.22	H	N	L	N	1.849	1.967	0.18
Fluconazole	3.04	0.90	N	N	N	N	2.384	1.006	0.465
DHγL acid	–25.56	0.21	N	N	N	N	1.951	3.075	–0.627
LNLD	–25.56	0.24	N	N	N	N	1.885	2.994	–0.497
OLC acid	–28.97	0.05	H	H	N	H	1.887	3.066	–0.445
ARQ acid	–25.22	0.18	N	N	N	N	1.933	3.291	–0.452
EST acid	–25.22	0.05	H	H	N	H	1.888	3.138	–0.392
MRG acid	–25.22	0.23	N	N	N	N	1.869	3.062	–0.348
PMT acid	–25.22	0.09	N	H	N	H	1.855	2.988	–0.293

DL: drug likeness; DS: drug score; Mu: mutagenicity; Tum: tumorigenicity; Rep: effects on the reproductive system Irrit: irritating effects; LD_{50}: oral rat acute toxicity; LOAEL: oral rat chronic toxicity; MRTD: maximum recommended tolerated dose. DHγL acid: dihomo-γ-linolenic acid; LNLD: linolelaidic acid; OLC acid: oleic acid; ARQ acid: arachidic acid; EST acid: stearic acid; MRG acid: margaric acid; PMT acid: palmitic acid. N: none; H: high; L: low.

may present toxicological alerts, side effects and adverse reactions (Table 3). Despite the presence of toxicological alerts for natural compounds, their antifungal potential can be explored in assays with isolated compounds and their proven toxicological profile in cell cultures and *in vivo* models.[48] Moreover, these compounds can be used as new strategies to combine natural products and fluconazole.[44,49]

Molecular dynamics

The 1-hydroxy-3,7-dimethoxyxanthone remained in the protein active site throughout simulation time (Figure S7, SI section). As shown, the interactions between the protein and the ligand do not significantly alter the stability of the 14-α-demethylase, and the flexibility of the amino acid residues changes little throughout the simulation (Figure S8, SI section). This stability of the protein in its APO conformation may be due to the presence of the Heme group, which is a very rigid structure capable of generating stability.[38] However, the permanence of the ligand on the site suggests that it establishes interactions sufficiently strong (Figure 2) to prevent the enzyme from performing its function.

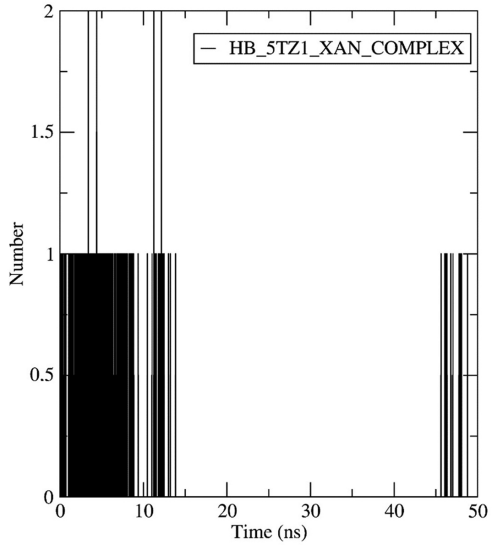

Figure 2. Molecular dynamics interactions for complex 1-hydroxy-3,7-dimethoxyxanthone and with amino acid residues of 14-α-demethylase site (5ZT1).

The evaluation of the results obtained from molecular dynamics tests between the xanthone and the fungal 14-α-demethylase protein revealed crucial information about the protein-ligand interaction. One notable observation is the constant permanence of the ligand in the protein active site throughout the simulation, as evidenced by the RMSD trajectory (Figure S7). This stable binding suggests a significant affinity between the compound and the enzyme active site. Furthermore, its intriguing to note that the interactions between the ligand and the protein do not cause significant disturbances in the structural stability of 14-alpha-demethylase, as indicated by the relatively small variation in the RMSF of the amino acid residues (Figure S8) throughout the simulation.[31]

A possible explanation for this conformational stability of the protein lies in the presence of the Heme group, which is known for its structural rigidity and ability to confer stability to the proteins that harbor it. The presence of Heme in 14-α-demethylase may be playing a fundamental role in maintaining the APO conformation of the enzyme during the interaction with the ligand (xanthone). However, despite the apparent structural stability, the continued presence of the ligand in the active site suggests that it establishes highly favorable interactions, as illustrated by the analysis of hydrogen bonds (Figure 2). In terms of energy, the protein in its conformation showed a greater deviation (Tot-Drift) in relation to the protein-binding complex, indicating that it has a more harmonious conformation (Table 4).[38]

Table 4. Molecular dynamics and RMSD analysis in the equilibrium state of the protein (14-alpha-demethylase site) in complex with 1-hydroxy-3,7-dimethoxyxanthone

	Energy / (kJ mol^{-1})		
	Average	RMSD	Tot-Drift
Coul-SR:Complex	−11.4 ± 0.69	6.7	2.1
Coul-SR:Protein_APO	−515.5 ± 4.2	31.3	−13.1
LJ-SR:complex	−221.9 ± 2.2	18.3	−11.8
LJ-SR:Protein_APO	−111.1 ± 3.7	12.2	−11.3

RMSD: root mean square deviation; Coul-SR: short-range Coulombic interaction energy; LJ-SR: short-range Lennard-Jones energy.

The persistence of the ligand in the active site throughout the simulation period suggests that these interactions are sufficiently strong to compromise the functional activity of 14-α-demethylase. The effective blocking of the active site by the xanthone could interfere with the enzyme ability to perform its catalytic function, with potential implications for fungal metabolism. Therefore, the results of this molecular dynamics study provide valuable insights into the mechanism of interaction between xanthone and 14-α-demethylase, highlighting the importance of molecular interactions in modulating enzymatic activity and offering a basis for future studies into the development of new natural antifungal drugs.

Conclusions

The phytochemical study of *B. brevifolia* leaf extracts using CC, GC-MS, GC-FID, NMR, and IR methods, allowed

the isolation and identification of a trioxygenated xanthone (1-hydroxy-3,7-dimethoxyxanthone), previously unheard of for the genus *Bredemeyera* Willd., and seven fatty acids (palmitic, margaric, linolelaidic, oleic, stearic, dihomo-γ-linolenic, and arachidic). All these substances have potential for the development of new antifungals obtained from natural sources. The integration of phytochemical data, *in vitro* and *in silico*, allowed to confirm the hypothesis that these compounds can behave as inhibitors, responsible for the activity on sterol-14-α-demethylase, important for the maintenance of fungal homeostasis and one of those responsible for the resistance to azole drugs (fluconazole). The use of computational chemistry tools (*in silico*) allowed to delineate a promising physicochemical, pharmacokinetic and toxicological profile for the development of new drugs through the evaluated compounds. Therefore, the results obtained in this research contribute to the chemical characterization and biological activity of the studied plant. The scarcity of previous studies regarding the chemical composition and the antifungal potential for this species makes it impossible to compare the results.

Supplementary Information

Supplementary data (Figures S1-S8, Tables S1-S4) are available free of charge at http://jbcs.sbq.org.br as PDF file.

Acknowledgments

The authors would like to thank Instituto Federal de Educação, Ciência e Tecnologia da Bahia, Universidade Estadual de Feira de Santana, Universidade Estadual do Sudoeste da Bahia, Universidade Federal do Pernambuco, UPCB Herbarium, LABAREMN/UFBA, CNPq, FAPESB and the Post-graduation Program in RGV. This study was financed in part by the Coordenação de Aperfeiçoamento de Pessoal de Nível Superior - Brasil - CAPES - Finance Code 001.

Author Contributions

Rubens S. Barreto was responsible for conceptualization, data curation, formal analysis, investigation, methodology, project administration, writing original draft, review and editing; Diego M. da Costa for formal analysis, investigation, methodology; Jailan S. Sousa for formal analysis, investigation, methodology, software; Vilisaimon S. de Jesus for formal analysis, investigation, methodology; Agnaldo P. da Silva for formal analysis, investigation, methodology; Maria Daniela S. Buonafina-Paz for formal analysis, investigation, methodology, writing original draft; Franz A. Graciano dos Santos for formal analysis, investigation, methodology, writing original draft; Rejane P. Neves for formal analysis, investigation, methodology, writing original draft; José Floriano B. Pastore for data curation, investigation, methodology; Bruno S. Andrade for formal analysis, investigation, methodology, software; Wagner R. de Assis Soares for formal analysis, investigation, methodology, software, writing original draft; Hugo Neves Brandão for conceptualization, formal analysis, funding acquisition, methodology; Clayton Q. Alves for conceptualization, data curation, formal analysis, funding acquisition, investigation, methodology, project administration, resources, supervision, writing original draft, review and editing; Rosane M. Aguiar for conceptualization, data curation, formal analysis, funding acquisition, investigation, methodology, project administration, resources, supervision, writing original draft, review and editing.

References

1. Lima, I. G.; Albuquerque, A. M. L.; Dias, A. C. A. A.; Loiola, M. I. B.; *Rodriguesia* **2018**, *69*, 673. [Crossref]
2. Macedo, J. G. F.; de Menezes, I. R. A.; Ribeiro, D. A.; Santos, M. O.; de Macêdo, D. G.; Macêdo, M. J. F.; de Almeida, B. V.; de Oliveira, L. G. S.; Leite, C. P.; Souza, M. M. A.; *J. Evidence-Based Complementary Altern. Med.* **2018**, *2018*, ID 6769193. [Crossref]
3. Daros, M. R.; Matos, F. J. A.; Parente, J. P.; *Planta Med.* **1996**, *62*, 523. [Crossref]
4. Pereira, B. M. R.; Daros, M. R.; Parente, J. P.; Matos, F. J. A.; *Phytother. Res.* **1996**, *10*, 666. [Crossref]
5. Silveira, E. R.; Falcão, M. J. C.; Menezes Jr., A.; Kingston, D. G. I.; Glass, T. E.; *Phytochemistry* **1995**, *39*, 1433. [Crossref]
6. de Oliveira, M. C. F.; Silveira, E. R.; *Phytochemistry* **2000**, *55*, 847. [Crossref]
7. Tene, M.; Tane, P.; Kuiate, J.-R.; Tamokou, J. D.; Connolly, J. D.; *Planta Med.* **2008**, *74*, 80. [Crossref]
8. Prasath, K. G.; Alexpandi, R.; Parasuraman, R.; Pavithra, M.; Ravi, A. V.; Pandian, S. K.; *Biomed. Pharmacother.* **2021**, *133*, 111043. [Crossref]
9. Muthamil, S.; Prasath, K. G.; Priya, A.; Precilla, P.; Pandian, S. K.; *Sci. Rep.* **2020**, *10*, 5113. [Crossref]
10. Narasimhan, S.; Maheshwaran, S.; Abu-Yousef, I. A.; Majdalawieh, A. F.; Rethavathi, J.; Das, P. E.; Poltronieri, P.; *Molecules* **2017**, *22*, 275. [Crossref]
11. Clinical and Laboratory Standards Institute (CLSI); *Reference Method for Broth Dilution Antifungal Susceptibility Testing of Yeasts, Approved Standard-Second Edition*, CLSI document M27-A3; CLSI: Pennsylvania, USA, 2008.
12. Clinical and Laboratory Standards Institute (CLSI); *Reference Method for Broth Dilution Antifungal Susceptibility Testing of Filamentous Fungi, Approved Standard*, CLSI document M38-A2; CLSI: Pennsylvania, USA, 2008.
13. *MarvinSketch*, version 6.2.3; ChemAxon Ltd., Budapest, Hungary, 2014. [Link] accessed in July 2024

14. Open Babel, version 3.1.1, http://openbabel.org, accessed in July 2024.
15. Protein Data Bank, Research Collaboratory for Structural Bioinformatics (RCSB), www.rcsb.org/, accessed in July 2024.
16. Eberhardt, J.; Santos-Martins, D.; Tillack, A. F.; Forli, S.; *J. Chem. Inf. Model.* **2021**, *61*, 3891. [Crossref]
17. *PyMOL Molecular Graphics System*, version 2.1, Schrödinger, LLC, USA, 2018.
18. *BIOVIA*, Discovery Studio, v. 4.5; Dassault Systèmes, San Diego, USA, 2021.
19. Sander, T.; Freyss, J.; von Korff, M.; Rufener, C.; *J. Chem. Inf. Model*. **2015**, *55*, 460. [Crossref]
20. Pires, D. E. V.; Blundell, T. L.; Ascher, D. B.; *J. Med. Chem*. **2015**, *58*, 4066. [Crossref]
21. Abraham, M. J.; Spoel, D. V. D.; Lindahl, E.; Hess, B.; GROMACS development team; *GROMACS*, version 2018; https://www.gromacs.org/, accessed in July 2024.
22. Brooks, B. R.; Brooks, C. L.; Mackerell Jr., A. D.; Nilsson, L.; Petrella, R. J.; Roux, B.; Won, Y.; Archontis, G.; Bartels, C.; Boresch, S.; Caflisch, A.; Caves, L.; Cui, Q.; Dinner, A. R.; Feig, M.; Fischer, S.; Gao, J.; Hodoscek, M.; Im, W.; Kuczera, K.; Lazaridis, T.; Ma, J.; Ovchinnikov, V.; Paci, E.; Pastor, R.W.; Post, C. B.; Pu, J. Z.; Schaefer, M.; Tidor, B.; Venable, R. M.; Woodcock, H. L.; Wu, X.; Yang, W.; York, D. M.; Karplus, M.; *J. Comput. Chem.* **2009**, *30*, 1545. [Crossref]
23. XMGRACE, version 5.1.25, https://plasmagate.weizmann.ac.il/Grace/, accessed in July 2024.
24. CGenFF interface, https://cgenff.umaryland.edu, accessed in July 2024.
25. Aberham, A.; Schwaiger, S.; Stuppner, H.; Ganzera, M.; *J. Pharm. Biomed. Anal.* **2007**, *45*, 437. [Crossref]
26. Feng, C.-Y.; Wu, Q.; Yin, D.-D.; Li, B.; Li, S. S.; Tang, Z. Q.; Xu, Y.-J.; Wang, L.-S.; *J. Pharm. Biomed. Anal.* **2018**, *161*, 455. [Crossref]
27. Aberham, A.; Pieri, V.; Croom Jr., E. M.; Ellmerer, E.; Stuppner, H.; *J. Pharm. Biomed. Anal.* **2011**, *54*, 517. [Crossref]
28. Feng, R.; Zhang, Y.-Y.; Chen, X.; Wang, Y.; Shi, J.-G.; Chem, C.-T.; Yeung, J. H. K.; Ma, J.-Y.; Tan, X.-S.; Yang, C.; Deng, Y.-L.; Zhang, Y.-K.; *J. Pharm. Biomed. Anal.* **2012**, *62*, 228. [Crossref]
29. Monte, F. J. Q.; Soares, F. P.; Braz-Filho, R.; *Fitoterapia* **2001**, *72*, 715. [Crossref]
30. Webster, D.; Taschereau, P.; Belland, R. J.; Sand, C.; Rennie, R. P.; *J. Ethnopharmacol.* **2008**, *115*, 140. [Crossref]
31. Keniya, M. V.; Sabherwal, M.; Wilson, R. K.; Woods, M. A.; Sagatova, A. A.; Tyndall, J. D. A.; Monk, B. C.; *Antimicrob. Agents Chemother.* **2018**, *62*, e01134-18. [Crossref]
32. Das, U. N.; *J. Adv. Res.* **2018**, *11*, 57. [Crossref]
33. Wang, Y.; Wang, S.; Zeng, L.; Han, Z.; Cao, J.; Wang, Y.; Zhong, G.; *Biochem. Biophys. Res. Commun.* **2021**, *585*, 82. [Crossref]
34. Alvarez-Rueda, N.; Fleury, A.; Logé, C.; Pagniez, F.; Robert, E.; Morio, F.; Pape, P. L.; *Med. Mycol.* **2016**, *54*, 764. [Crossref]
35. Rosam, K.; Monk, B. C.; Lackner, M.; *J. Fungi* **2021**, *7*, 1. [Crossref]
36. Altieri, C.; Cardillo, D.; Bevilacqua, A.; Sinigaglia, M.; *J. Food Prot.* **2007**, *70*, 1206. [Crossref]
37. Anyanwu, G. O.; Ur-Rehman, N.; Onyeneke, C. E.; Rauf, K.; *J. Ethnopharmacol.* **2015**, *175*, 648. [Crossref]
38. Hargrove, T. Y.; Friggeri, L.; Wawrzak, Z.; Qi, A.; Hoekstra, W. J.; Schotzinger, R. J.; York, J. D.; Guengerich, F. P.; Lepesheva, G. I.; *J. Biol. Chem.* **2017**, *292*, 6728. [Crossref]
39. Zhang, J.; Li, L; Lv, Q.; Yan, L.; Wang, Y.; Jiang, Y.; *Front. Microbiol.* **2019**, *10*, 691. [Crossref]
40. Lipinski, C. A.; *Adv. Drug Delivery Rev.* **2016**, *101*, 34. [Crossref]
41. Gomez-Lopez, A.; *Clin. Microbiol. Infect.* **2020**, *26*, 1481. [Crossref]
42. Cheng, F.; Li, W.; Zhou, Y.; Shen, J.; Wu, Z.; Liu, G.; Lee, P. W.; Tang, Y.; *J. Chem. Inf. Model.* **2012**, *52*, 3099. [Crossref]
43. Bellmann, R.; Smuszkiewicz, P.; *Infection* **2017**, *45*, 737. [Crossref]
44. Srivastava, D.; Yadav, A.; Naqvi, S.; Awasthi, H.; Fatima, Z.; *Curr. Pharm. Des.* **2022**, *28*, 1703. [Crossref]
45. Kalaimathi, K.; Rani, J. M. J; Manogar, P.; Vijayakumar, S.; Prakash, N.; Karthikeyan, K.; Thiyagarajan, G.; Bhavani, K.; Prabhu, S.; *Integr. Med. Rep.* **2022**, *1*, 76. [Crossref]
46. Słoczyńska, K.; Pękala, E.; Wajda, A.; Węgrzyn, G., Marona, H.; *Lett. Appl. Microbiol.* **2010**, *50*, 252. [Crossref]
47. Wang, W.-Y.; Cai, H.-Q.; Qu, S.-Y.; Lin, W.-H.; Liang, C.-C.; Liu, H.; Xie, Z.-X.; Yuan, Y.-J.; *Biomolecules* **2022**, *12*, 845. [Crossref]
48. Hornik, C. D.; Bondi, D. S.; Greene, N. M.; Cober, M. P.; John, B.; *J. Pediatr. Pharmacol. Ther.* **2021**, *26*, 115. [Crossref]
49. Haji, M. H.; Mohamed, A. B.; Albashir, A. A.; Mirghani, M.; *Eur. J. Med. Plants* **2022**, *33*, 16. [Crossref]

Submitted: March 5, 2024
Published online: August 9, 2024